Who needs population inversion? Automatically phase-matched quantum coherence contributions as a source for THz radiation

Inès Waldmueller, Weng W. Chow and Michael C. Wanke

Sandia National Laboratories, Albuquerque, New Mexico 87185, USA

Phone:+1-505-845-2058, Fax:+1-505844-3211, Email: iwaldmu@sandia.gov

Abstract—We investigate the capabilities of an optically-pumped, electronically-driven terahertz quantum cascade laser. Due to automatically phase-matched quantum coherence contributions, the laser can operate both with and without population inversion between the lasing subbands. The latter is especially convenient for operating at higher temperatures, where fast relaxation mechanisms detrimentally effect the population inversion.

I. INTRODUCTION

Medical imaging, homeland security, spectroscopy and satellite telecommunications are some of the reasons for the substantial interest in compact and efficient sources for THz radiation. As quantum cascade lasers (QCLs) have already been proven to be reliable sources over a wide range of infrared frequencies, the idea of THz-QCLs seems promising [1]. However, to date, THz-QCLs have exhibited low wall-plug efficiencies, on the order of only 1%, and are restricted to low-temperature operation [e.g. [3]].

For this reason, we investigated the feasibility of an optically-pumped, electrically-driven THz-QCL (OPED-QCL) scheme [2]. As we will show, OPED-QCLs cannot only generate THz radiation via stimulated emission, but also via automatically phase-matched quantum coherence contributions.

The approach uses the advantages of optical conversion, the most important of which is high temperature operation. In contrast to typical optical conversion [e.g. [4],[6]], the THz energy is not derived from the external optical field, but comes from the forward electrical bias as in a current-driven QCL. As a result, we circumvent the fundamental constraint to optical conversion efficiency (the Manley-Rowe limit).

The central features of an OPED-QCL are sketched in Fig. 1. Via an external optical field, carriers are excited from subband 1 to subband 2. Lasing transitions between subbands 2 and 3 generate the desired THz radiation. Crucial to the approach is the design of the coupled quantum wells so that under lasing conditions (i.e. in the presence of strong optical nonlinearities and many-body effects) the transition frequencies between subbands 1 and 2, and subbands 3 and 4 are sufficiently similar for the same external optical field to simultaneously populate the higher laser subband (2) and deplete the lower laser subband (3). The latter not only enables the desired recovery of the pump photons via stimulated emission, but also offers the interesting possibility of externally
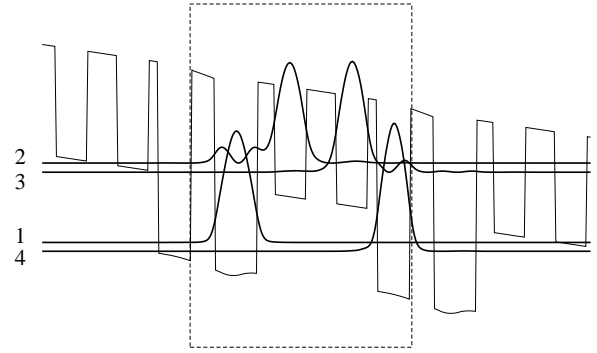

Fig. 1. Conduction band profile and moduli squared of the central wavefunctions calculated using a self-consistent Schrödinger and Poisson solver. The four-well module grown in GaAs.$Al_{0.4}Ga_{0.6}As$ and $Al_{0.15}Ga_{0.85}As$ is outlined by the dashed box. Gap energies and dipole moments are given by $E_{23} = E_{14} = 16.5$ meV, $E_{21} = E_{34} = 144$ meV, $d_D = d_{12} = d_{34} = 0.9$ nm, $d_{23} = 1.4$ nm.

controlling the depopulation of the lower laser subband.

The capabilities of the scheme are demonstrated via the intensities of the two optical fields (THz field and drive field), which can be determined by solving Maxwell's wave equations for the fields:

$$(\nabla^2 + \frac{n^2}{c^2}\frac{\partial^2}{\partial t^2})E_i(r,t) = -\mu_0\frac{\partial^2}{\partial t^2}P_i(r,t) \,. \quad (1)$$

Here $E_i(r,t) = \tilde{E}_i e^{-i\,\omega_i t} + c.c$ denotes THz and drive field with complex amplitudes $\tilde{E}_i$. The material response has been divided into a resonant part, treated dynamically in terms of the macroscopic optical polarizations P_i (determined by the respective intersubband coherences p_{ij}),

$$P_{\mathbf{THz}} = d_{23}\,p_{23}\,e^{i\,\omega_{\mathbf{THz}}t} + c.c. \,, \quad (2)$$

$$P_{\mathbf{D}} = (d_{12}\,p_{21} + d_{34}\,p_{34})\,e^{i\,\omega_{\mathbf{D}}t} + c.c. \,, \quad (3)$$

and a nonresonant part, which is lumped in with the (background) refractive index n.

For continuous-wave (cw) excitation, the corresponding intersubband coherences can be expressed in terms of the

subband populations n_i:

$$p_{23} = \mathrm{i}\, d_{23} \tilde{E}_{\mathbf{THz}}^* \Big[\frac{(n_2 - n_3)(d_{23}^2 |\tilde{E}_{\mathbf{THz}}|^2 + 4\gamma)}{2\gamma(4d_D^2 |\tilde{E}_D|^2 + d_{23}^2 |\tilde{E}_{\mathbf{THz}}|^2 + 4\gamma^2)}$$

$$+ \frac{d_D^2 |\tilde{E}_D|^2 (n_1 + n_2 - n_3 - n_4))}{2\gamma(4d_D^2 |\tilde{E}_D|^2 + d_{23}^2 |\tilde{E}_{\mathbf{THz}}|^2 + 4\gamma^2)} \Big] , \quad (4)$$

$$p_{21} + p_{34} = -2\mathrm{i}\, d_D \tilde{E}_{\mathbf{D}}^* \frac{(n_1 - n_2 - n_3 + n_4)\gamma}{d_{23}^2 |\tilde{E}_{\mathbf{THz}}|^2 + 4\gamma^2} . \quad (5)$$

d_{23} denotes the dipole moment between the lasing subbands 2 and 3, $d_D = d_{12} = d_{34}$ the dipole moments between subbands 1 and 2, and 3 and 4, respectively [see also Fig. 1] and γ the dephasing of the intersubband coherences. Note that for simplicity we give only the special results for an OPED-QCL with equal dipole moments between subbands 1,2 and 3,4.

The first term in Eq. (4) accounts for the possible generation of THz radiation via stimulated emission. Being linearly dependent on the population difference between the lasing subbands, this contribution only generates THz radiation if the necessary condition of population inversion is fulfilled. However, with increasing temperature, achieving and maintaining the necessary population inversion is increasingly complicated by non-radiative carrier losses.

The second term in Eq. (4) accounts for quantum coherence effects, i.e. interactions of the THz field with intersubband coherences induced by dipole-forbidden transitions ($1 \leftrightarrow 3$ and $2 \leftrightarrow 4$) which are additional sources for THz radiation. For the design presented in Fig. 1, these contributions depend on the drive field only through its intensity and are consequently automatically phase-matched to the THz field. In addition, the quantum coherence contributions yield THz radiation whenever the subband populations fulfill the condition $n_1 + n_2 - n_3 - n_4 > 0$, a condition which allows lasing without population inversion between the lasing subbands. An example for THz generation without population inversion is presented in Fig. 2.

Equation (5) shows the possibility to recover the pump photons in our scheme. Fulfilling the conditions for maximum drive recovery, i.e. $n_1 - n_2 - n_3 + n_4 \equiv 0$, yields optimal conversion efficiency. In this case all the THz energy comes from the forward electrical bias and the drive intensity is completely recycled. However, if all carriers are located in the lasing subbands, i.e. $n_2 + n_3 \equiv N$ with N being the total number of carriers, the conversion efficiency reaches its minimum. The drive field gets depleted.

Besides analyzing the possibilities of optimizing the experimental configuration based on Eqs. 1-5, simulations are also performed to determine the sensitivity to design changes involving, ratio of dipole moments, transition energies and sample dimensions.

II. Conclusion

In summary, we present a scheme for efficient and high temperature THz generation. The scheme is also interesting in terms of providing a practical experimental platform of demonstrating quantum coherence effects. A microscopic theory is
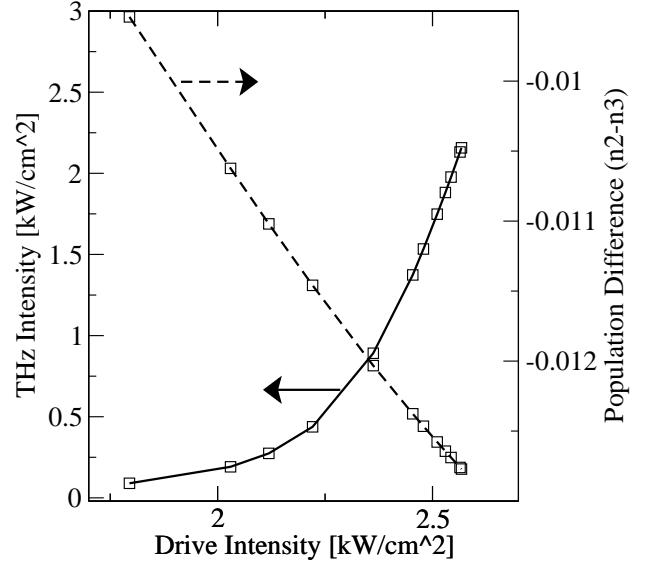

Fig. 2. Dependence of THz drive intensity and population inversion on drive intensity for the QCL shown in Fig. 1. Due to quantum coherence contributions [see Eq. 4], it is possible to generate THz radiation without population inversion.

used to arrive at an optimum laser design which is currently being fabricated.

References

[1] R. Köhler, A. Tredicucci, F. Beltram; H.E. Beere, E. H. Linfi eld, A. G. Davies, D. A. Ritchie, R. C. Iotti, F. Rossi, "Terahertz semiconductor-heterostructure laser", *Nature* vol. 417, pp. 156-159, May 2002.
[2] I. Waldmueller, M. C. Wanke, and W. W. Chow, "Exceeding the Manley-Rowe quantum effi ciency limit in an optically pumped THz amplifier," submitted to Phys. Rev. Lett.
[3] S. Kumar, B. S. Williams, S. Kohen, Q. Hu, and J. L. Reno, "Continuous-wave operation of terahertz quantum-cascade lasers above liquid-nitrogen temperature," *Appl. Phys. Lett*, vol. 84, pp. 2494-2496, Apr. 2004.
[4] O. Gauthier-Lafaye, F. H. Julien, S. Cabaret, J. M. Lourtioz, G. Strasser, E. Gornik, M. Helm, P. Bois, "High-power GaAs/AlGaAs quantum fountain unipolar laser emitting at 14.5 mu m with 2.5
[5] H. C. Liu, I. W. Cheung, A. J. SpringThorpe, C. Dharma-wardana, Z. R. Wasilewski, D. J. Lockwood, and G. C. Aers, "Intersubband Raman Laser," *Appl. Phys. Lett.*, vol. 78, pp. 3580-3582, Jun. 2001.
[6] H. C. Liu, C. Y. Song, Z. R. Wasilewski, A. J. SpringThorpe, J. C. Cao, C. Dharma-wardana, G. C. Aers, D. J. Lockwood, and J. A. Gupta, "Coupled Electron-Phonon Modes in Optically Pumped Resonant Intersubband Lasers," *Phys. Rev. Lett.*, vol. 90, pp. 0774021-0774024, Feb. 2003